Modelling and control of actuators with built-in position controller

Zilong Shao, Gang Zheng, Denis Efimov, Wilfrid Perruquetti

Modelling and control of actuators with built-in position controller

Zilong SHAO [*,**] **Gang Zheng** [*,**] **Denis Efimov** [*,**]
Wilfrid Perruquetti [*,**]

[*] *CRIStAL (UMR CNRS 9189) Ecole Centrale de Lille,Cité Scientifique, 59651, Villeneuve d'Ascq, France*
[**] *Non-A team at Inria Lille Nord Europe, Parc Scientifique de la Haute Borne, 40 Avenue Halley, 59650 Villeneuve dAscq (e-mail: zilong.shao, gang.zheng, denis.efimov, wilfrid.perruquetti@inria.fr)*

Abstract: This paper addresses the set-point control of actuators integrated with built-in controller, which presents steady-state error (SSE) under certain load. To eliminate the SSE, a model of the actuator-plus-controller system is established and identified, a switched adaptive controller is developed to work with the embedded one, considering the physical constraints, a switching control strategy is proposed. Implementation of the proposed controller and control strategy shows the ability of error elimination and the robustness under different operational conditions, with comparison to classic integral controller.

1. INTRODUCTION

Nowadays the low-cost hobby actuators existing in the market become popular with researchers, engineers and hobbyists. This kind of non-industrial actuator is relatively cheap, small and light, but with high output torque, thus can be mounted into manipulators, humanoid robots, hexapods, etc. Besides, to be more user-friendly, some of these actuators provide a built-in micro-controller, so the desired position can be set directly as input, this renders the actuators position-controlled and relieves the users from controller design. However, apart from these advantages, several operational constraints or drawbacks as below may also exist:

• Torque saturation. For the driving circuit of an actuator, the current is usually limited in case of burning out components, and this current limit generates the limit of the output torque for the actuators.

• Velocity and acceleration limitation. Due to physical limitations and protection for the components, the velocity and acceleration are limited as well.

• Non-robust built-in controller. Built-in controller allows users to control easily the actuators by setting directly a desired position. However, in some cases, the performance with that controller cannot be satisfactory.

• Impossibility of torque control. Due to the built-in controller, it is generally the desired position which is taken directly as input. Since the torque is calculated by the built-in controller, thus computed-torque based controller cannot be implemented.

• Not enough sensors. Due to small size and low price, few sensors are integrated, thus few feedbacks are available. Besides, the sensor precision and output data rate (ODR) are largely limited.

To improve the performance of this kind position-controlled actuators, works have been done to provide position controlled robots with torque control capability, since torque controlled robots are preferred to achieve high performance. In [Khatib et al. (2008)], a torque-position transformer for position controlled robots is introduced, with which desired joint torque is converted into instantaneous increments of joint position inputs, this approach has been implemented on the Honda ASIMO robot arm. However, this transformer is based on the total knowledge of the built-in controller, which, designed by the manufacturer of the actuators, is usually unknown or partly unknown to individual users.

This paper is motivated by such kind of actuators, embedded with built-in controller which presents SSE. The main contribution of this paper is the proposal of an adaptive controller and switching control strategy, and experimental validation of its improvement over a classic integral controller.

The rest of this paper is organized as follows. In Section II, we introduce the actuator and analyse the SSE. Control strategy, modelling and identification of the system will be presented in Section III. Section IV is devoted to the design of the proposed adaptive controller. Section V includes experimental results of the proposed controller with comparison to an integral controller. Conclusion and perspectives will be given in Section VI.

2. INTRODUCTION OF THE ACTUATOR AND ANALYSIS OF THE SSE

2.1 Introduction of the actuator

The studied actuator is Dynamixel AX-12A actuators as shown in Fig. 1. Under joint mode, the angle range of the actuator is limited between 0° and 300°. This angular range is scaled between 0 and 1024 (Fig. 2) with a resolution of 0.29°.

This actuator is equipped with a built-in controller with which the desired position can be taken directly as input, a feedback of current position is available. The working mechanism of the whole actuator system (built-in controller plus physical plant) can be concluded in Fig. 3. u is the input for the system, which is the desired position x_d for a set-point regulation problem, x is the current position which serves as the output and feedback,

Fig. 1. AX-12A actuator

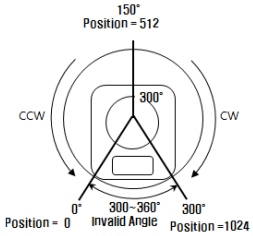

Fig. 2. Angle range

may be corrupted by noise, $e = u - x$ denotes the position error, τ is the generated torque determined by the built-in controller based on e.

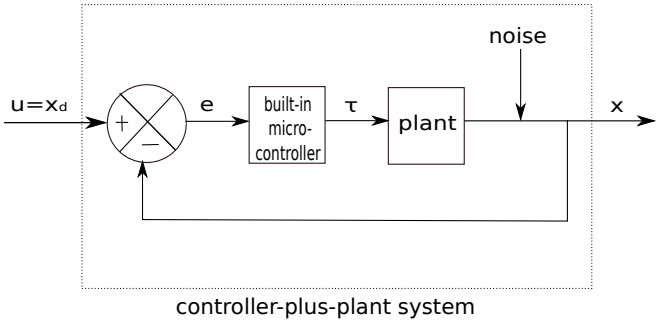

Fig. 3. Working mechanism of the whole actuator system

However, steady-state errors when applying the built-in controller are observed with a load on the actuator which will be investigated in the following section.

2.2 Analysis of the SSE

For the built-in controller, Fig. 4 describes the compliance between the output torque limit (noted as τ_l) and the position error. We note output torque limit instead of output torque, because some other constraints may exist (for example velocity saturation), in this case, the actual output torque should not exceed the limit, otherwise the actual output torque is the limit.

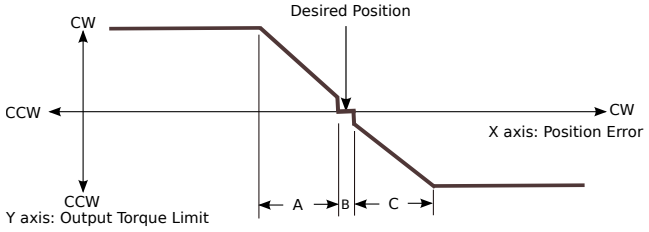

Fig. 4. Compliance of the built-in controller

To dig up, we start with the position error e outside the zone $A \bigcup C$ (B can be ignored since $A = C = 64 \times 0.29°$ and $B = 1 \times 0.29°$), $\tau = \tau_l$ and τ_l is saturated at the maximal value, this leads to a phase of acceleration. When the velocity attains its maximal value and afterwards keeps constant at this value, τ equals no longer τ_l, but the value which maintains a zero acceleration, this leads to a zero-acceleration phase during witch $|\tau| \leq |\tau_l|$. After $A \bigcup C$ is entered, as $|e|$ decreases, $|\tau_l|$ decreases persistently and will "meet" τ again, since then $\tau = \tau_l$ and $|\tau|$ decrease with $|\tau_l|$, thus zero-acceleration can no longer be maintained and this leads to a deceleration phase until finally

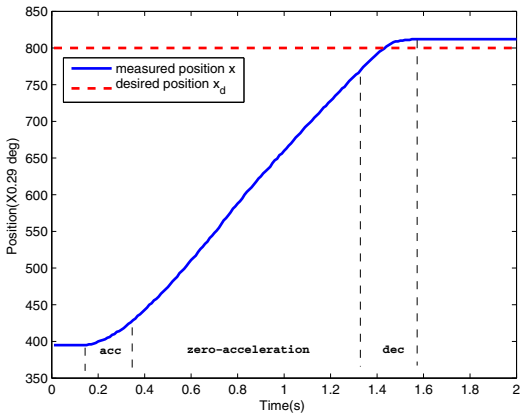

Fig. 5. A trajectory with SSE under built-in controller

stopping. This analysis corresponds to the trajectory shown in Fig. 5.

Within $A \bigcup C$, τ_l decreases proportionally with e. So during the deceleration phase, τ ($=\tau_l$) can be approximately considered as proportional to e, thus it is a proportional controller which is unable to eliminate steady-state error. When a load torque is presented on the rotational axis, to be balanced finally, a certain τ should be produced to balance the load torque and static friction, this certain τ is based on a certain e, this is where the SSE comes from.

3. CONTROL STRATEGY, MODELLING AND IDENTIFICATION

3.1 Switched control strategy

To seek a solution to eliminate the SSE, following constraints of the studied actuator should be taken into account:

- The built-in controller cannot be avoided;
- Both the built-in controller model and the plant model are largely unknown;
- The output torque is saturated and the saturation bound is unknown;
- The computed-torque based control laws cannot be performed since the input is desired position;
- Among the feedbacks of interest, only the current position feedback is reliable [1].

We cannot control τ directly, but we can control it indirectly by controlling u, instead of keeping u constant to x_d, we introduce an auxiliary controller which outputs u based on desired position x_d and feedback current position x. Considering the velocity saturation, this auxiliary controller is switched on only during the deceleration phase. For this, let us firstly define a neighbourhood Ω around the desired position x_d:

$$\Omega = \{x : |x - x_d| \leq \omega\},$$

where x represents the current position of the actuator, and ω is a pre-defined switching region, freely chosen by us, which is desired to slightly contain the whole deceleration phase. Outside of this region, i.e. $x \notin \Omega$, we use only the built-in

[1] Velocity and load are measured with a frequency 4 times smaller than position and the load is used only to detect in which direction the force works.

controller, of which the advantage is the rapidity because either torque or velocity is saturated; within this region, we activate this auxiliary controller which generates intermediate desired position u_2. Therefore, the switched control strategy proposed in this paper can be summarized as follows:

$$u = \begin{cases} x_d, & \text{if } x \notin \Omega \\ u_2, & \text{if } x \in \Omega \end{cases} \tag{1}$$

This switched control strategy is described in Fig. 6. Since it is difficult to detect when exactly the deceleration starts, ω can be practically chosen to be the zone $A \bigcup C$ (B can be ignored).

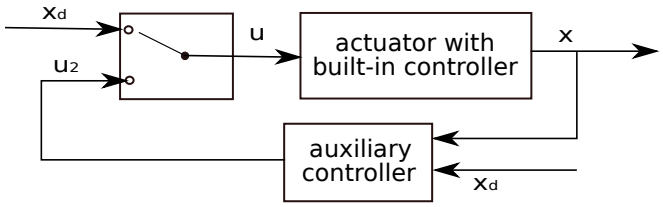

Fig. 6. Switched control strategy

As for the design of the auxiliary controller, an integral controller with a constant gain K_i described as

$$u = K_i \int (x_d - x), \tag{2}$$

may be a simple choice, since it does not need a precise model of the system or any derivative of the measured position, however, an integral term with a constant gain may not be suitable for a nonlinear and time-varying actuator system, from performance viewpoint. For more robust performance, a model-based controller might be better. For this, we should firstly have a model.

3.2 Modelling during deceleration phase

Consider a rigid body driven by a torque, rotates about its axis of rotation, the dynamic model of the system can be described as follows:

$$\tau = I\ddot{x} + F_v\dot{x} + Q(x), \tag{3}$$

where x is the angular position and τ is the torque exerted on the body; I is the moment of inertia of the body and F_v is the viscous friction coefficient; $Q(x)$ stands for the load gravity torque, which is generally a trigonometric function of x.

For the studied actuator, during the deceleration phase, the output torque τ ($=\tau_l$) obeys the compliance shown in Fig. 4, thus can be considered as a function of the position error $u-x$:

$$\tau = f(u-x), \tag{4}$$

(3) and (4) bring

$$f(u-x) = I\ddot{x} + F_v\dot{x} + Q(x), \tag{5}$$

which is equivalent to:

$$\ddot{x} = -\frac{F_v}{I}\dot{x} - \frac{Q(x)}{I} + \frac{f(u-x)}{I}. \tag{6}$$

By writing the right hand side of (6) as a sum of a linear part and a nonlinear part, it yields

$$\ddot{x} = -a_1(t)x - a_2(t)\dot{x} + k(t)u + \lambda(t), \tag{7}$$

where λ represents the modelling errors and disturbances.

As the range of the deceleration phase is largely limited, we can consider $a_1(t)$, $a_2(t)$, $k(t)$ and $\lambda(t)$ as slowly time-varying parameters within certain range, in what follows, we are going to estimate a linear nominal model of (7) with constant parameters $\bar{a}_1$, $\bar{a}_2$, $\bar{k}$.

3.3 Identification of the linear nominal parameters

Considering a linear nominal model of (7) as follows:

$$\ddot{x} = -\bar{a}_1 x - \bar{a}_2\dot{x} + \bar{k}u, \tag{8}$$

where $\bar{a}_1$, $\bar{a}_2$, $\bar{k}$ are constant. (8) can be rewritten in the following matrix form:

$$\ddot{x} = \begin{bmatrix} x & \dot{x} & u \end{bmatrix} \begin{bmatrix} -\bar{a}_1 & -\bar{a}_2 & \bar{k} \end{bmatrix}^T. \tag{9}$$

Denoting $A = \begin{bmatrix} \ddot{x}(t_1) \\ \ddot{x}(t_2) \\ \vdots \\ \ddot{x}(t_n) \end{bmatrix}$, $B = \begin{bmatrix} x(t_1) & \dot{x}(t_1) & u(t_1) \\ x(t_2) & \dot{x}(t_2) & u(t_2) \\ \vdots & \vdots & \vdots \\ x(t_n) & \dot{x}(t_n) & u(t_n) \end{bmatrix}$ and $C = \begin{bmatrix} -\bar{a}_1 & -\bar{a}_2 & \bar{k} \end{bmatrix}^T$, then we can use least square method to estimate those parameters in C:

$$C = (B^TB)^{-1}B^TA. \tag{10}$$

It is worth noting that the above method is based on the knowledge of the velocity $\dot{x}$ and the acceleration $\ddot{x}$, since we have only reliable measurement of the current position x, therefore, we need to estimate $\dot{x}$ and $\ddot{x}$ by using some robust differentiators, which will be analysed in the following.

3.4 Comparison of differentiators

Let $y(t) = x(t) + w(t)$ be a noisy observation of a signal $x(t)$ where $w(t)$ represents the noise, and we need to estimate the ith order derivative of $x(t)$. For this, a large amount of literatures about high-order differentiation have been published, like High-Gain differentiator [Dabroom and Khalil (1997), Dabroom and Khalil (1999)], higher-order sliding modes differentiator (HOSM) [Levant (2003), Efimov and Fridman (2011)], homogeneous finite-time differentiator (HOMD) [Dabroom and Khalil (1997), Perruquetti et al. (2008)], algebraic-based differentiator (ALIEN) [Fliess et al. (2008), Mboup et al. (2007)]. The following gives a brief recall of them.

ALIEN differentiator The basic idea of this approach is to approximate the noisy signal by a suitable polynomial during a small time window. In a practical way, the first-order and second-order derivative estimates can be expressed as:

$$\hat{\dot{y}}(t) = -\frac{6}{T}\int_0^1 (1-2\tau)y(t-\tau T)d\tau, \tag{11}$$

$$\hat{\ddot{y}}(t) = \frac{60}{T^2}\int_0^1 (6\tau^2 - 6\tau + 1)y(t-\tau T)d\tau, \tag{12}$$

where y is the signal and T is the window size.

High-Gain, HOSM and HOMD differentiators The recursive schemes of the High-Gain, HOSM and HOMD differentiators are of a similar formulation, which can be described as follows:

$$
\begin{aligned}
\dot{z}_1 &= -k_1 \ulcorner z_1 - y \lrcorner^{\alpha} + z_2 \\
&\vdots \\
\dot{z}_i &= -k_i \ulcorner z_1 - y \lrcorner^{i\alpha-(i-1)} + z_{i+1} \\
&\vdots \\
\dot{z}_{n-1} &= -k_{n-1} \ulcorner z_0 - y \lrcorner^{(n-1)\alpha-(n-2)} + z_n \\
\dot{z}_n &= -k_n \ulcorner z_0 - y \lrcorner^{n\alpha-(n-1)}
\end{aligned} \tag{13}
$$

where $\ulcorner a \lrcorner^b = |a|^b sign(a)$ and k_i is the chosen gain. Then z_i represents the estiamteion of the ith order derivative of y. According to Dabroom and Khalil (1997), there are three cases:

- $\alpha = 1$, (13) represents a High-Gain differentiator;
- $\alpha \in (\frac{n-1}{n}, 1)$, (13) represents a HOMD differentiator;
- $\alpha = \frac{n-1}{n}$, (13) represents a HOSM differentiator.

Comparison of the performance The performance of these four differentiators is shown in Fig. 7 for a trajectory under the built-in controller. From the results we can see that the ALIEN differentiator is robust to noise because of its integration on a time window, but it presents time delay in real time, however this can be solved by a proper shift afterwards, so we choose ALIEN differentiator for off-line differentiation for the purpose of the parameter identification in (9). For controller's need, the HOMD differentiator is taken to do on-line differentiation because it presents less chattering and quicker convergence than High-Gain and HOSM differentiator.

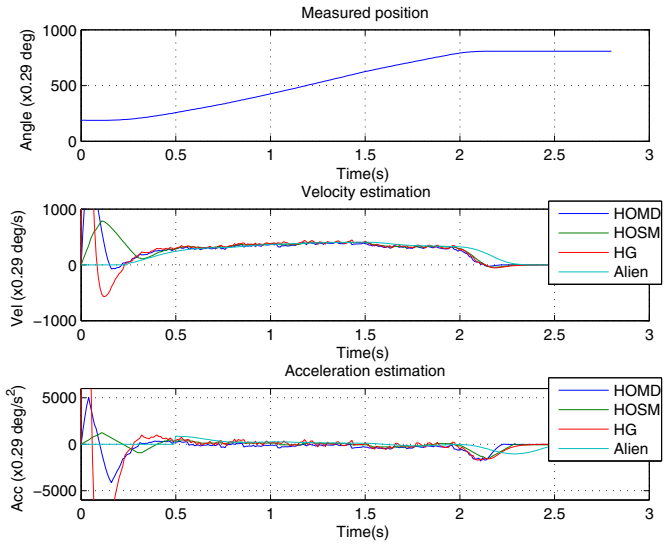

Fig. 7. Velocity and acceleration estimates

4. ADAPTIVE CONTROLLER DESIGN

Suppose that the precise model of the actuator during the deceleration phase is the nominal model (8) with the uncertainties of the parameters as follows:

$$\ddot{x} = -\bar{a}_1 x - \bar{a}_2 \dot{x} + \bar{k}(u + \varphi^T \theta), \tag{14}$$

where $\bar{a}_1, \bar{a}_2, \bar{k}$ are the identified parameters of the nominal model (8), and

$$\varphi = \begin{bmatrix} x \\ \dot{x} \\ u \\ 1 \end{bmatrix}, \theta = \begin{bmatrix} (\bar{a}_1 - a_1(t))/\bar{k} \\ (\bar{a}_2 - a_2(t))/\bar{k} \\ (k(t) - \bar{k})/\bar{k} \\ \lambda(t)/\bar{k} \end{bmatrix},$$

where θ represents the bounded unknown piece-wise constant uncertainties of the parameters.

Set $X = \begin{bmatrix} x \\ \dot{x} \end{bmatrix}$, then (14) can be written as:

$$\dot{X} = AX + B(u + \varphi^T \theta), \tag{15}$$

where $A = \begin{bmatrix} 0 & 1 \\ -\bar{a}_1 & -\bar{a}_2 \end{bmatrix}$ and $B = \begin{bmatrix} 0 \\ \bar{k} \end{bmatrix}$, we suppose A is Hurwitz.

To stabilize (17), suppose the *control law* is of the following form [Åström and Wittenmark (2013)]:

$$u = -\varphi^T \hat{\theta}, \tag{16}$$

where $\hat{\theta}$ stands for the estimate of θ, will be derived hereafter.

Note $\tilde{\theta} = \theta - \hat{\theta}$, then (16) becomes

$$\dot{X} = AX + B\varphi^T \tilde{\theta}. \tag{17}$$

By choosing the following Lyapunov Function candidate as:

$$V = X^T P X + \tilde{\theta}^T \gamma^{-1} \tilde{\theta}, \tag{18}$$

where P is a positive definite symmetric matrix and $\gamma > 0$, so V is positive definite. The time derivative of V equals:

$$\dot{V} = X^T (PA + A^T P) X + 2(X^T P B \varphi^T + \gamma^{-1} \dot{\tilde{\theta}}^T) \tilde{\theta}. \tag{19}$$

Defining a positive-definite, symmetric matrix Q that satisfies the Lyapunov equation

$$Q = -(PA + A^T P), \tag{20}$$

and taking

$$\dot{\tilde{\theta}} = -\gamma \varphi B^T P X, \tag{21}$$

then (19) becomes:

$$\dot{V} = -X^T Q X \leq 0. \tag{22}$$

We now detail the stability for X. Since $\dot{V}$ is negative semi-definite and V is lower bounded by zero, V remains upper bounded in the time interval $[0, +\infty)$. Since V is upper bounded, it is obvious from the definition of V given in (18) that X and $\tilde{\theta}$ are bounded, which also means that x, $\dot{x}$ and $\hat{\theta}$ are bounded. Now, from (16), u is bounded since u depends only on the bounded quantities x, $\dot{x}$ and $\hat{\theta}$. Since u is bounded, (15) shows that $\dot{X}$ is bounded. Since $\dot{X}$ is bounded, we can state from (22) that $\dot{V}$ which depends only on X and $\dot{X}$ is bounded. Therefore, since V is lower bounded by zero, $\dot{V}$ is negative semi-definite, and $\dot{V}$ is bounded, then by Barbalat's lemma,

$$\lim_{t \to +\infty} \dot{V} = 0, \tag{23}$$

which means that by the Rayleigh-Ritz Theorem

$$\lim_{t \to +\infty} \lambda_{min}\{Q\} \|X\|^2 = 0, \tag{24}$$

where $\lambda_{min}\{Q\}$ is the minimal eigenvalue of Q. As $\lambda_{min}\{Q\} > 0$, it is clear from (24) that

$$\lim_{t \to +\infty} X = 0. \tag{25}$$

Finally, by recalling that the actual unknown parameter θ is piece-wise constant, i.e., $\dot{\theta} = 0$, we obtain the *adaptive update rule* for $\hat{\theta}$ as

$$\dot{\hat{\theta}} = -\dot{\tilde{\theta}} = \gamma \varphi B^T P X. \tag{26}$$

Remark 1. The *control law* (16) and the *adaptive update rule* (26) are used for the stabilization task. In tracking problem X should be replaced by the error vector and (16) should be changed to $u = \bar{k}^{-1}(\bar{a}_1 x_d + \bar{a}_2 \dot{x}_d + \ddot{x}_d) - \varphi^T \hat{\theta}$.

5. EXPERIMENTAL VALIDATION

5.1 Experiment description

Our experiment testbed is the manipulator PhantomX Pincher [2], which is mounted by 5 AX-12A actuators, as shown in Fig. 8. As this paper targets the control of single actuator, we activate one actuator and keep the others fixed. Since the SSE is introduced by the gravity load torque on the actuator, and the load torque depends on the load weight and the load configuration, several scenarios of configuration are considered and additional loads are attached to the end-effector to change the weight. For the estimation of the parameters of the nominal model, the studied actuator operates under the built-in controller. To validate the proposed controller, auxiliary integral controller and adaptive controller are implemented. The sampling frequency is 100Hz. In this paper, only the experimental results of the third actuator is presented.

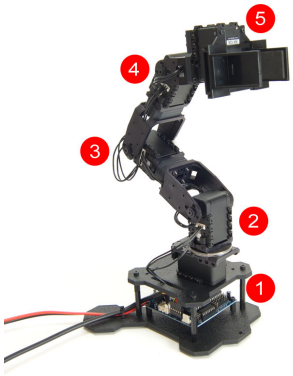

Fig. 8. Experimental manipulator

5.2 Identification results

The ALIEN differentiator is performed to get the estimates of the velocity and acceleration. Then the model parameters can be estimated according to (10).

As a result, we obtain the nominal model of the actuator as below:

$$\ddot{x} = -120.2x - 15.2\dot{x} + 118.1u, \tag{27}$$

where $A = \begin{bmatrix} 0 & 1 \\ -120.2 & -15.2 \end{bmatrix}$ is Hurwitz.

5.3 Controller performance

The comparison of the performance with only built-in controller, with addition of integral controller and with addition of adaptive controller under two different scenarios is shown from Fig. 9 to Fig. 12.

With only built-in controller, the SSE cannot be eliminated and the amplitude of the SSE differs from final position, meanwhile, additional load increases the SSE amplitude. However, with addition of either integral controller or adaptive controller, the SSE vanishes for all scenarios.

For integral controller, it works well without additional load (Fig. 9(b)), as the integral gain is tuned in this scenario, for other configurations or with the additional load, overshoot appears and convergence time increases significantly. As for adaptive controller, it works perfectly for all the listed cases, with quick convergence and nearly no overshoot.

6. CONCLUSIONS

For our studied actuator, the proposed adaptive controller shows powerful ability of error elimination , and improved performance under different operational conditions compared to integral controller. As for the next step, we will generate this idea to the whole introduced 5-DOF manipulator of which the dynamical model is highly coupling.

REFERENCES

Åström, K.J. and Wittenmark, B. (2013). *Adaptive control*. Courier Dover Publications.

Dabroom, A. and Khalil, H.K. (1997). Numerical differentiation using high-gain observers. In *Decision and Control, 1997., Proceedings of the 36th IEEE Conference on*, volume 5, 4790–4795. IEEE.

Dabroom, A.M. and Khalil, H.K. (1999). Discrete-time implementation of high-gain observers for numerical differentiation. *International Journal of Control*, 72(17), 1523–1537.

Efimov, D.V. and Fridman, L. (2011). A hybrid robust nonhomogeneous finite-time differentiator. *sign*, 1(1.5), 1–5.

Fliess, M., Join, C., and Sira-Ramirez, H. (2008). Non-linear estimation is easy. *International Journal of Modelling, Identification and Control*, 4(1), 12–27.

Khatib, O., Thaulad, P., Yoshikawa, T., and Park, J. (2008). Torque-position transformer for task control of position controlled robots. In *Robotics and Automation, 2008. ICRA 2008. IEEE International Conference on*, 1729–1734. IEEE.

Levant, A. (2003). Higher-order sliding modes, differentiation and output-feedback control. *International journal of Control*, 76(9-10), 924–941.

Mboup, M., Join, C., Fliess, M., et al. (2007). A revised look at numerical differentiation with an application to nonlinear feedback control. In *The 15th Mediterrean Conference on Control and Automation-MED'2007*.

Perruquetti, W., Floquet, T., and Moulay, E. (2008). Finite-time observers: application to secure communication. *Automatic Control, IEEE Transactions on*, 53(1), 356–360.

[2] http://www.trossenrobotics.com/p/PhantomX−Pincher−Robot−Arm.aspx

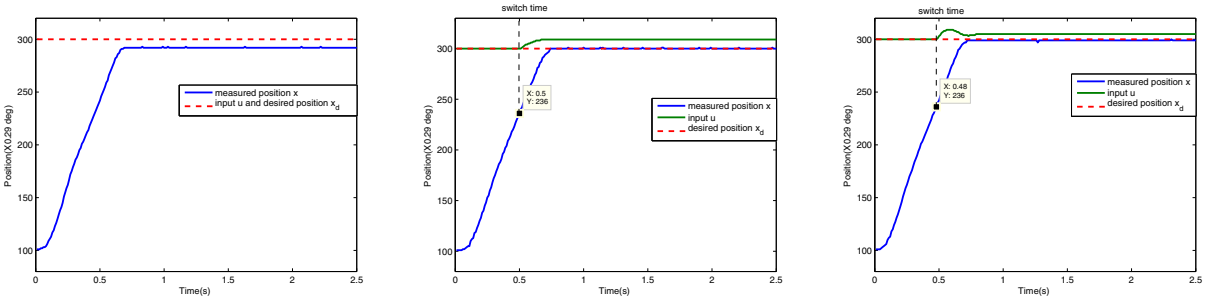

(a) Only built-in controller (b) Addition of integral controller (c) Addition of adaptive controller

Fig. 9. Scenario A without additional load

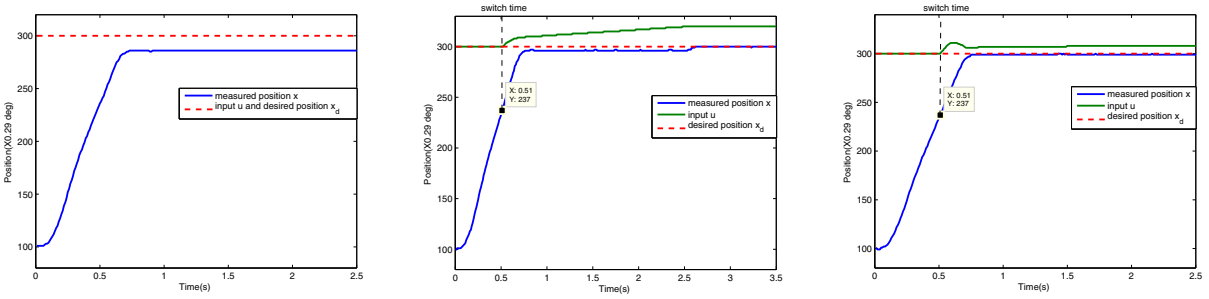

(a) Only built-in controller (b) Addition of integral controller (c) Addition of adaptive controller

Fig. 10. Scenario A with additional load

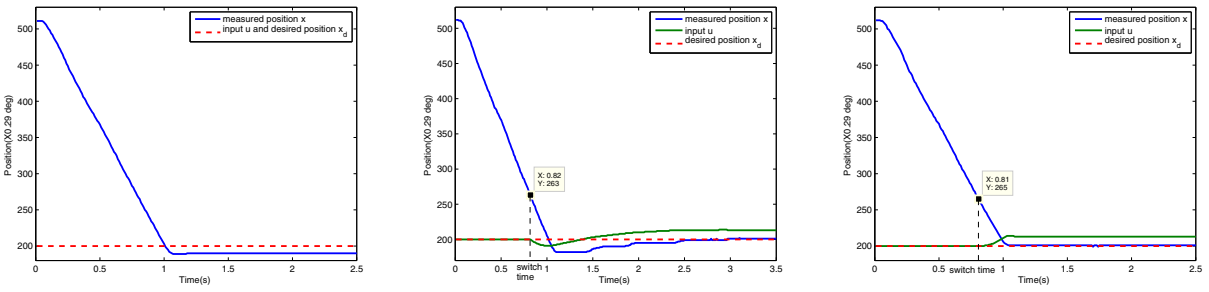

(a) Only built-in controller (b) Addition of integral controller (c) Addition of adaptive controller

Fig. 11. Scenario B without additional load

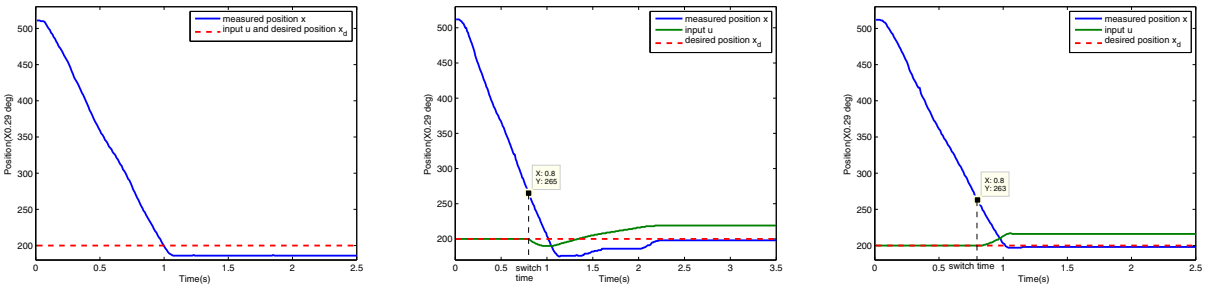

(a) Only built-in controller (b) Addition of integral controller (c) Addition of adaptive controller

Fig. 12. Scenario B with additional load